Gazi University Journal of Science
GU J Sci
25(1):9-17 (2012)

ORIGINAL ARTICLE

Band Structure and Optical Properties of BiOCl: Density Functional Calculation

Husnu KOC[1♠], Harun AKKUS[2], Amirullah M. MAMEDOV[3]

[1]*Siirt University, Vocational Schools, Güres street, 56100 Siirt, Turkey*
[2]*Physics Department, Yuzuncu Yil University, 65080 Van, Turkey*
[3]*Physics Department, Cukurova University, Adana, Turkey*

Received:06/06/2010 Revised: 24/11/2010 Accepted:27/02/2011

ABSTRACT
The electronic band structures, density of states (DOS) and optical properties of BiOCl Crystal are investigated using the density functional theory under the local density approximation (LDA). The obtained electronic band structure show that BiOCl crystal has an indirect forbidden band gap of 2.45 eV. The structural optimization for BiOCl has been performed using the LDA. The result of the structure optimization of BiOCl have been compared with the experimental results and have been found to be in good agreement with these results. The linear photon-energy dependent dielectric functions and some optical properties such as the energy-loss function, the effective number of valence electrons and the effective optical dielectric constant are calculated.

Keywords: BiOCl, Ab-inito, band structure, optical properties.

1. INTRODUCTION

Bismuth oxychloride (BiOCl), a member of compounds with the general formula $A_m^V B_n^{VI} X_p^{VII}$ ($A = As, Sb, Bi; B = O, S, Se$ and $X = Cl, Br, I$) is a wide bandgap semiconductor with a tetragonal PbFCl-type structure (space group P_4/nmm: No:129) [1,2]. This crystal has 2 BiOCl molecules in a unit cell. Therefore, this compound has a complex structure with 18 valence electrons per unit cell.

The unit cell of BiOCl is shows in Figure 1 [3] and atomic positions in the unit cell are given in Table 1 [1]. The crystal structure can derive from the fluorite (CaF_2) structure. The Bi atom is coordinated to a square antiprism with four O atoms in one base and four Cl atoms in another. The O atom is tetrahedrally coordinated to four Bi atoms. The Cl atom is bonded with four Bi atom in a planar square to form a pyramid and with its nonbonding (lone pair) electrons pointing to the other side of the square. As shown in the Figure 1, the (BiOCl) layers are stacked together by the nonbonding (van der Waals) interaction through the Cl atoms along the c- axist. Therefore, the structure is not closely packed in this direction [3].

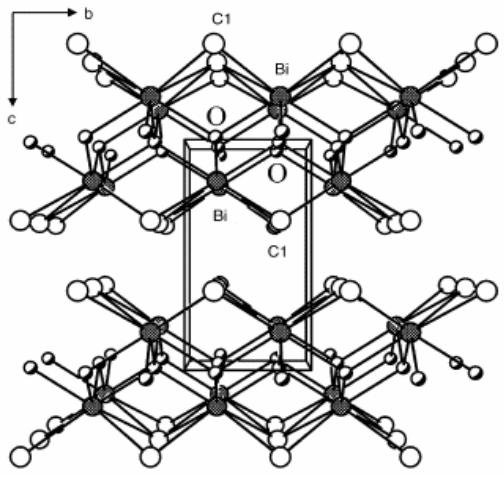

Figure 1. The unit cell of BiOCl viewed along (100) [3].

♠Corresponding author, e-mail: hkoc@student.cu.edu.tr

Table 1. Fractional atomic coordinates (Å) for BiOCl [1]

Atoms	x	y	z
Bi	0.250000	0.250000	0.1714(3)
	0.750000	0.750000	0.828600
O	0.250000	0.750000	0.000000
	0.750000	0.250000	0.000000
Cl	0.250000	0.250000	0.6459(25)
	0.750000	0.750000	0.354100

The electronic structure of BiOCl has been calculated via the tight-binding linear muffin-tin orbital (TB-LMTO) method within the local density approximation (LDA) by Zhang et al. [3] The indirect nature calculated is in agreement with the linear relationship observed experimentally between $(\alpha E)^{1/2}$ and E (where α and E represent the absorption coefficient and photon energy, respectively), although the calculated band gap is relatively narrow [3]. The electronic band structure of BiOX (X=F, Cl, Br and I) have been calculated via DFT method within GGA scheme by Huang at al. [4]. The atomic charges and bond orders have been analyzed using the Mulliken population analysis [5-7], and the spatial distribution of orbital density has also been described [4]. As far as we know, no ab initio general potential calculations of the optical properties of BiOCl have been reported in detail.

In the present work, we have investigated the electronic band structure, the total density of states (DOS), structure optimization and photon energy-dependent optical properties of the BiOCl crystal using a pseudopotential method based on the density functional theory (DFT) in the local density approximation (LDA) [8].

2. COMPUTATIONAL DETAILS

SIESTA (The Spanish Initiative for Electronic Simulations with Thousands of Atoms) code [9-10] was utilized in this study to calculate the energy spectra and optical of BiOCl. It solves the quantum mechanical equation for the electron within DFT approach in the LDA parameterized by Ceperley and Alder [11]. The interactions between electrons and core ions are simulated with seperable Troullier – Martins [12] norm-conserving pseudopotential. The basis set is based on the finite range pseudoatomic orbitals (PAO's) of the Sankey-Nicklewsky type [13], generalized to include multiple-zeta decays.

We have generated atomic pseudopotentials separately for Bi, O and Cl by using the $6s^26p^3$, $2s^22p^4$ and $3s^23p^5$ atomic configurations, respectively. The cut-off radii for present atomic pseudopotentials are taken as s: 3.82 au, p: 2.71 au, d: 2.92au, f: 2.92 au for Bi, 1.43 au for the s, p, d and f channels of O and s: 1.62 au, P: 1.62 au, d:1.84 au, f: 1.84 au for Cl.

SIESTA calculates the self-consistent potantial on a grid in real space. The fineness of this grid is determined in terms of an energy cut-off E_c in analogy to the energy cut-off when the basis set involves plane waves. Here by using a double-zeta plus polarization (DZP) orbitals basis and the cut-off energies between 50 and 450 Ry with various basis sets, we found an optimal value of around 300 Ry for BiOCl. For the final computations, 98 k-points for BiOCl were found to be adequate for obtaining the total energy with an accuracy of about $1\ meV/atoms$.

3. RESULTS AND DISCUSSION

3.1. Structural Optimization

All physical properties are related to the total energy. For instance, the equilibrium lattice constant of a crystal is the lattice constant that minimizes the total energy. If the total energy is calculated, any physical property related to the total energy can be determined. Firstly, the equilibrium lattice parameter was computed by minimizing the crystal's total energy calculated for the different values of lattice constant by means of Murnaghan's equation of states (EOS) [14] as in Figure 2, and the result are shown in Table 2 along with the experimental and theoretical values. The lattice parameters for BiOCl are found to be a=b=3.88 (Å) and c=7.314 (Å) for tetragonal structures, and it are in a good agreement with the experimental and theoretical values. In all our calculations we have used the computed lattice parameter.

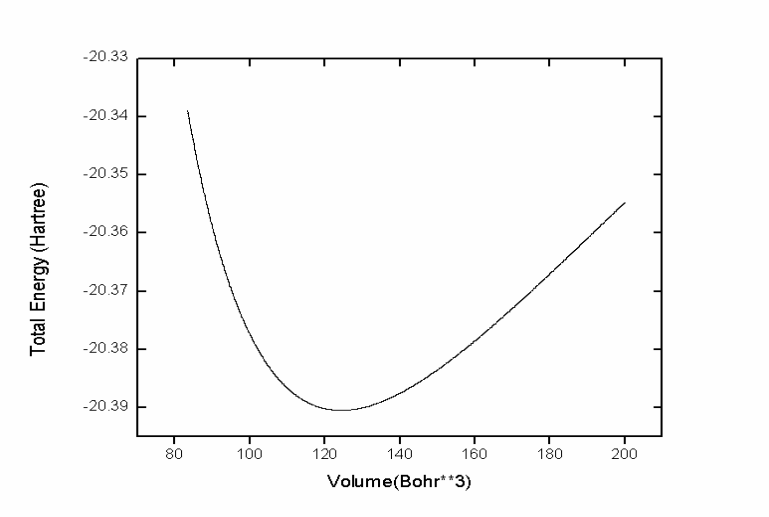

Figure 2**.** Energy versus volume curve of BiOCl.

Table 2. Structure parameters of BiOCl materials.

Reference	a (Å)	c (Å)	Space Group
Present	3.888	7.314	
Experimental [1]	3.887	7.354	
Experimental [15]	3.888	7.357	P_4/nmm
Experimental [3]	3.890	7.890	
Theory [4]	3.824	7.243	

3.2. Electronic Band Structure

The electronic band structures of BiOCl crystals have been calculated along high symmetry directions in the first Brillouin zone (BZ) of the tetragonal system and are shown in Figure 3. The band structures were calculated along the special lines connecting the high-symmetry points Γ (1/2,0,0), X (1/2,0,0), Z(0,0,1/2), M(1/2,1/2,0), R(1/2,0,1/2) and A(1/2,1/2,1/2) in the k-space.

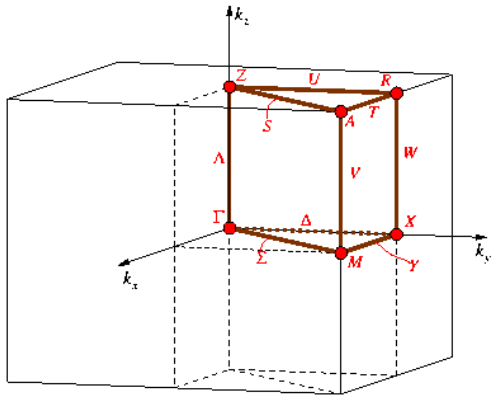

Figure 3. First Brillouin zone for BiOCl (space group P_4/nmm).

The results of the calculations are shown in Figure 4 for BiOCl crystal. In the rightmost panels of this figure, the density of states (DOS) are presented. The calculated band gap values of these crystals are given in Table 3. The valence band in our calculations is composed of the 3s and 3p -states of the Cl, the 2s and 2p –states of the O atom, and the 6s –states of the Bi atom, while the conduction band consists of the 6p –states of the Bi atom.

Table 3. Energy band gaps for BiOCl.

Referance	$E_g(eV)$
Present	2.45 indirect- 2.77 direct
Experimental [3]	3.46 indirect
Theory [4]	2.59 indirect

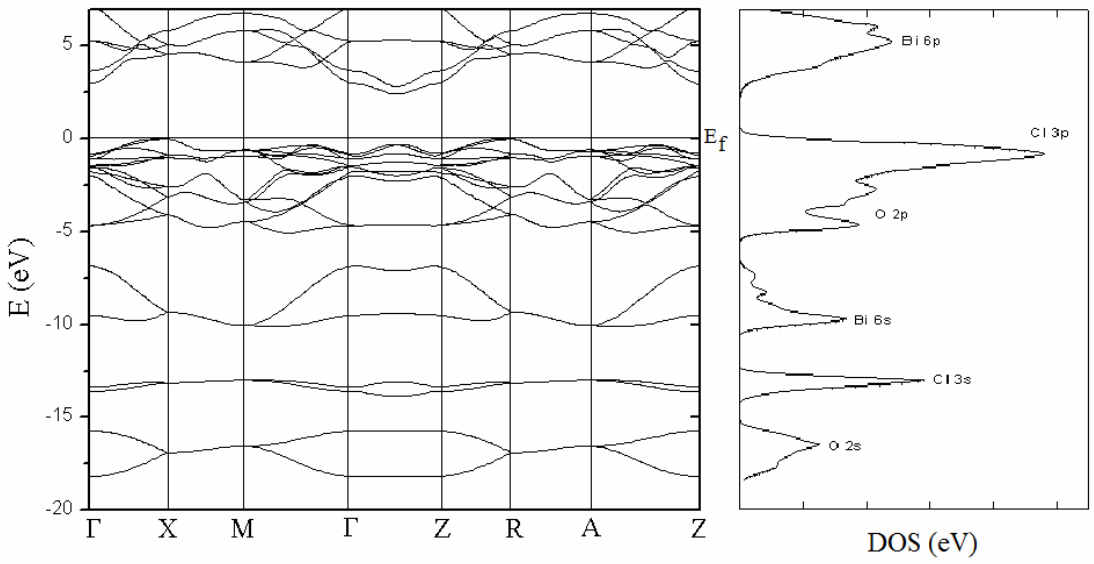

Figure 4**.** Energy band structure and DOS (density of states) for BiOCl.

As can be seen in Figure 4, The top of the valence band positioned near the R point between the Z-R points, and the bottom of the conduction band is located at the nearly midway between the Γ and Z points of the BZ. The band gap of BiOCl is thus indirect with the value 2.45 eV. For BiOCl, the lowest direct band gap value obtained is 2.77 eV.

Finally, the band gap values obtained for BiOCl are less than measured values. For all crystal structures considered, the band gap values are underestimated than the experimental values. This state is caused from the exchange-correlation approximation of DFT.

3.3. Optical Properties

It is well known that the effect of the electric field vector, $\mathbf{E}(\omega)$, of the incoming light is to polarize the material. At the level of linear response this polarization can be calculated using the following relation [16]:

$$P^i(\omega) = \chi_{ij}^{(1)}(-\omega,\omega).E^j(\omega), \tag{1}$$

Where $\chi_{ij}^{(1)}$ is the linear optical susceptibility tensor and it is given by [17]

$$\chi_{ij}^{(1)}(-\omega,\omega) = \frac{e^2}{\hbar\Omega}\sum_{nm\vec{k}} f_{nm}(\vec{k})\frac{r_{nm}^i(\vec{k})r_{mn}^i(\vec{k})}{\omega_{mn}(\vec{k})-\omega} = \frac{\varepsilon_{ij}(\omega)-\delta_{ij}}{4\pi} \tag{2}$$

Where n,m denote energy bands, $f_{mn}(\vec{k}) \equiv f_m(\vec{k}) - f_n(\vec{k})$ is the fermi occupation factor, Ω is the normalization volume. $\omega_{mn}(\vec{k}) \equiv \omega_m(\vec{k}) - \omega(\vec{k})$ are the frequency differences, $\hbar\omega_n(\vec{k})$ is the energy of band n at wavevector **k.** The $\vec{r}_{nm}$ are the matrix elements of the position operator and are give by

$$r_{nm}^i(\vec{k}) = \frac{v_{nm}^i(\vec{k})}{i\omega_{nm}}; \quad \omega_n \neq \omega_m \tag{3}$$

$$r_{nm}^i(\vec{k}) = 0; \quad \omega_n = \omega_m$$

Where $v_{nm}^i(\vec{k}) = m^{-1}p_{nm}^i(\vec{k})$, m is the free electron mass, and $\vec{p}_{nm}$ is the momentum matrix element.

As can be seen from equation (2), the dielectric function $\varepsilon_{ij}(\omega) = 1 + 4\pi\chi_{ij}^{(1)}(-\omega,\omega)$ and the imaginary part of $\varepsilon_{ij}(\omega)$, $\varepsilon_2^{ij}(\omega)$, is given by

$$\varepsilon_2^{ij}(w) = \frac{e^2}{\hbar\pi}\sum_{nm}\int d\vec{k} f_{nm}(\vec{k})\frac{v_{nm}^i(\vec{k})v_{nm}^j(\vec{k})}{\omega_{mn}^2}\delta(\omega-\omega_{mn}(\vec{k})). \quad (4)$$

The real part of $\varepsilon_{ij}(\omega), \varepsilon_1^{ij}(\omega)$, can be obtained by using the Kramers-Kroning transformation

$$\varepsilon_1^{ij}(\omega)-1 = \frac{2}{\pi}\wp\int_0^\infty \frac{\omega'\varepsilon_2^{ij}(\omega')}{\omega'^2-\omega^2}d\omega'. \quad (5)$$

Because the Kohn-Sham equations determine the ground state properties, the unoccupied conduction bands as calculated have no physical significance. If they are used as single-particle states in a calculation of optical properties for semiconductors, a band gap problem comes into included in calculations of response. In order to take into account self-energy effects, in the present work, we used the 'scissors approximation' [16].

In the present work, Δ, the scissor shift to make the theoretical band gap match the experimental one, is 1.01 eV for BiOCl.

Expressions for the energy-loss spectrum, $L(\omega)$

$$L_{ij}(\omega) = -\operatorname{Im}\varepsilon_{ij}^{-1}(\omega), \quad (6)$$

The known sum rules [18] can be used to determine some quantitative parameters, particularly the effective number of the valence electrons per unit cell N_{eff}, as well as the effective optical dielectric constant ε_{eff}, which make a contribution to the optical constants of a crystal at the energy E_0. One can obtain an estimate of the distribution of oscillator strengths for both intraband and interband transitions by computing the $N_{eff}(E_0)$ defined according to

$$N_{eff}(E) = \frac{2m\varepsilon_0}{\pi\hbar^2 e^2 Na}\int_0^\infty \varepsilon_2(E)EdE, \quad (7)$$

Where N_a is the density of atoms in a crystal, e and m are the charge and mass of the electron, respectively and $N_{eff}(E_0)$ is the effective number of electrons contributing to optical transitions below an energy of E_0.

Further information on the role of the core and semi-core bands may be obtained by computing the contribution which the various bands make to the static dielectric constant, ε_0.

According to the Kramers-Kronig relations, one has

$$\varepsilon_0(E)-1 = \frac{2}{\pi}\int_0^\infty \varepsilon_2(E)E^{-1}dE. \quad (8)$$

One can therefore define an 'effective' dielectric constant, which represents a different mean of the interband transitions from that represented by the sum rule, equation (8), according to the relation

$$\varepsilon_{eff}(E)-1 = \frac{2}{\pi}\int_0^{E_0} \varepsilon_2(E)E^{-1}dE. \quad (9)$$

The physical meaning of ε_{eff} is quite clear: ε_{eff} is the effective optical dielectric constant governed by the interband transitions in the energy range from zero to E_0, i.e. by the polarizition of the electron shells.

In order to calculate the optical response by using the calculated band structure, we have chosen a photon-energy range of 0-30 eV and have seen that a 0-18 eV photon-energy range is sufficient for most optical functions.

The BiOCl crystal has an tetragonal structure that is optically uniaxial system. For this reason, the linear dielectric tensor of the BiOCl crystal has two independent components that are the diagonal elements of the linear dielectric tensor. The calculated real parts and imaginary parts of the xx- and zz- components of the linear frequency- dependent dielectric function are presented in Figure 5. The function ε_1^{xx} is equal to zero at about 6.66 eV, 10.72 eV, 13.90 eV, 22.5 eV, 22.99 eV and 23.23 eV (at the W, X, Y, Z, U and V in Figure 5), while the other function ε_1^{zz} is equal to zero at about 7.37 eV, 8.35 eV, 8.49 eV, 9.90 eV, 12.97 eV and 22.28 eV (at the W, X, Y, Z, U and V in Figure 5). The values of the ε_2^{xx} and ε_2^{zz} peaks shown in Figure 5 are summarized in Table 4. This peaks correspond to the transitions from the valence to the conduction band (see Figure 5).

Table 4. Comparative characteristics of linear optical functions of BiOCl crystal.

Peak (eV)																
ε_2	A	B	C	D	E	F	G	H	I	J	K	L	M	N	O	P
xx	5.44	6.39	7.21	11.53	12.49	13.49	14.93	15.61	16.21	17.66	18.47	18.93	20.73	21.95	22.91	24.02
zz	4.97	6.04	7.26	8.65	10.39	12.87	14.06	15.02	15.51	16.29	17.85	18.93	19.59	20.21	23.61	24.87

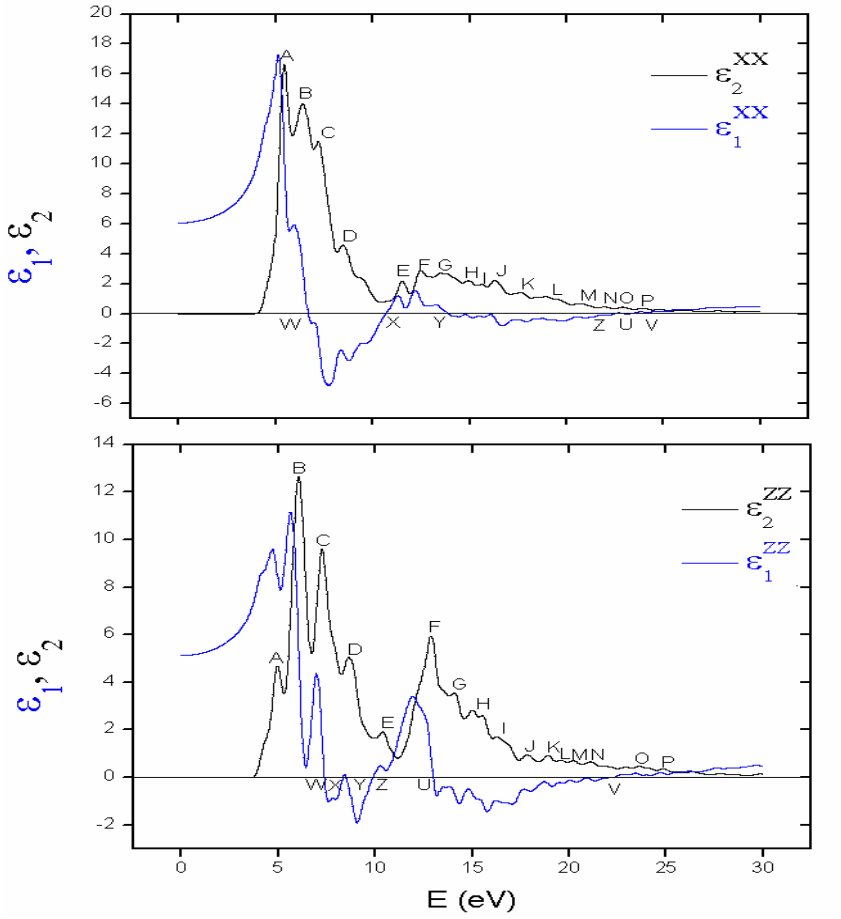

Figure 5. Energy spectra of dielectric function $\varepsilon = \varepsilon_1 - i\varepsilon_2$ for BiOCl.

The calculated energy-loss functions, $L(\omega)$, are presented in Figure 6. In this figure, L_{xx} and L_{zz} correspond to the energy-loss functions along the x- and z- directions, respectively. The function $L(\omega)$ describes the energy loss of fast electrons traversing the material. The sharp maxima in the energy-loss function are associated with the existence of plasma oscillations [19]. The curves of L_{xx} and L_{zz} in Figure 6 have a maximum near 24.33 and 25.23 eV, respectively and these value coincide with the V point in Figure 5.

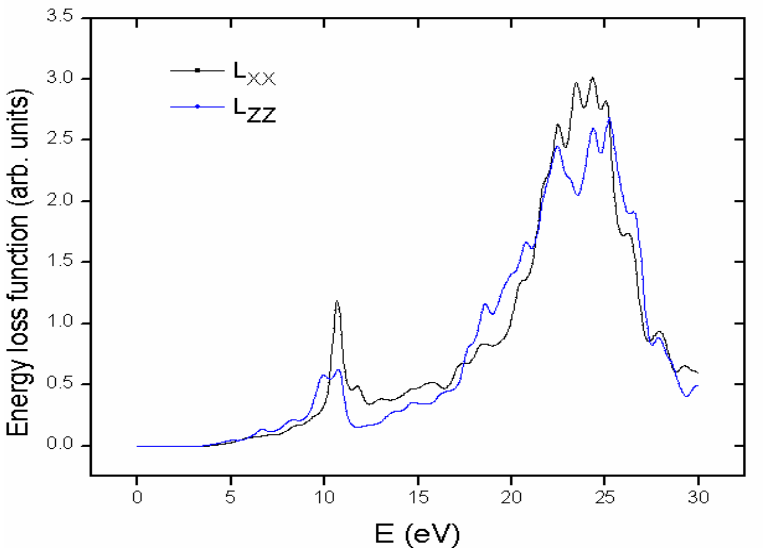

Figure 6. Energy-loss function along the x- and z- axes for BiOCl

The calculated effective number of valence electrons (N_{eff}) and the effective dielectric constant (ε_{eff}) are given in Figure 7. The effective number of valence electron per unit cell, N_{eff}, contributing in the interband transitions, reaches saturation value at about 26 eV. This means that deep-lying valence orbitals paticipate in the interband transitions as well (see Figure 4)

The effective optical dielectric constant, ε_{eff}, shown in Figure 7, reaches a saturation value at about 16 eV.

The photon-energy dependence of ε_{eff} can be separated into two regions. The first is characterized by a rapid rise and it extends up to 10 eV. In the second region the value of ε_{eff} rises more smoothly and slowly and tends to saturation at the energy 16 eV. This means that the greatest conribution to ε_{eff} arises from interband transitions between 4.7 and 16 eV.

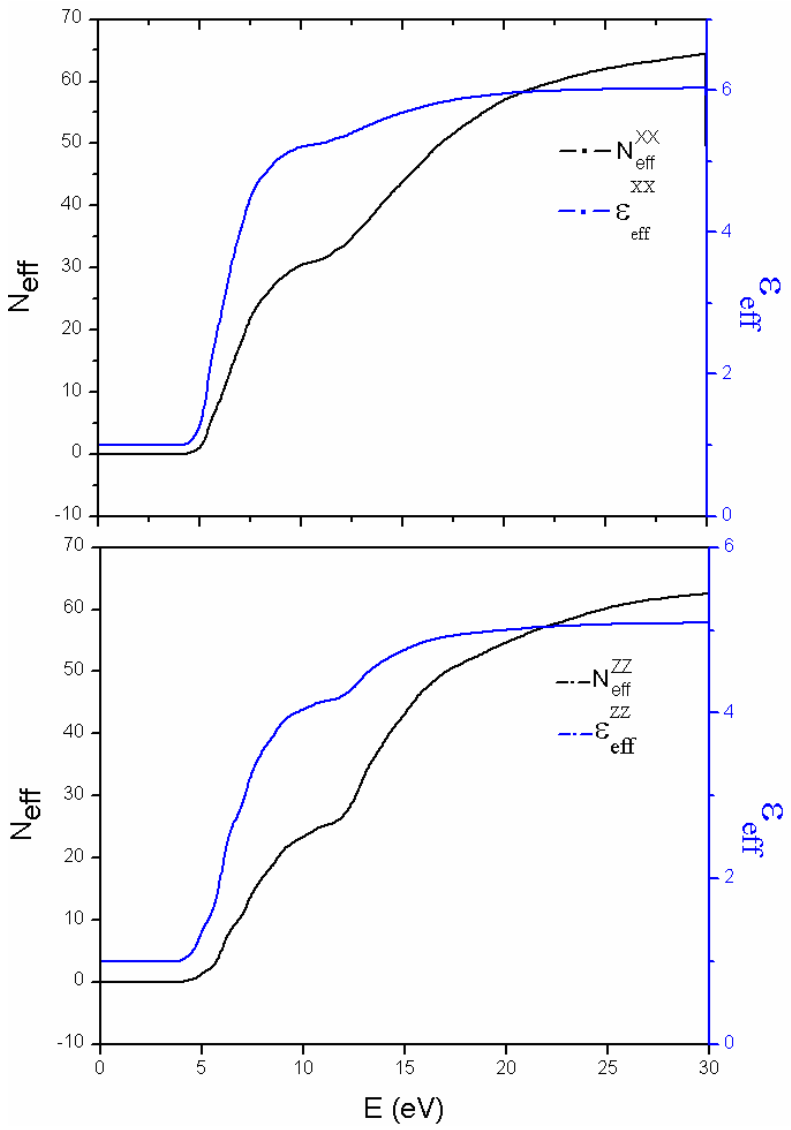

Figure 7. Energy spectra of N_{eff} and ε_{eff} along the x- and z- axes.

4. CONCLUSIONS

In present work, we have made a detailed investigation of the electronic structure and frequency-dependent linear optical properties of the BiOCl crystal using the density functional methods. The task of this work was to apply the density-functional methods to a complex crystal like the BiOCl. It is seen that BiOCl crystal have the indirect forbidden gap. The obtained band gap values are in agreement with the previous results. The total DOS calculation shows that the valence band is composed of 3s and 3p states of the Cl atom, 2s and 2p states of the O atom and 6s states of the Bi atom while the conduction band consists of 6p states of the Bi atom. we have examined photon energy dependent dielectric functions as well as related quantities such as energy-loss function, the effective number of valence electrons per unit cell participating in the interband transitions and the effective optical dielectric function along the x- and z- axes. The results of the structural optimization implemented using the LDA are in excellent agreement with the experimental results. To our knowledge, this is the first detailed study of the optical properties of BiOCl.

REFERENCES

[1] Keramidas, K.G., Voutsas, G.P., and Rentzeperis, P.I., "The crystal structure of BiOCl", ***Z. Kristallogr***. 205: 35-40, (1993).

[2] Peng, H., Chan, C.K., Meister, S.M., Zhang, X.F., and Cui,Y., "Shape evolution of layer-structured bismuth oxychloride nanostructures via low-temperature chemical vapor transport", ***Chem. Mater***. 21: 247-252, (2009.

[3] Zhang, K.-L., Liu, C.-M., Huang, F.-Q., Zheng, C., and Wang, W.-D., "Study of the electronic structure and photocatalytic activity of the BiOCl photocatalyst", ***Applied Catalysis B: Environmental*** 68: 125-129, (2006).

[4] Huang, W.L., and Zhu, Q., "DFT calculations on the electronic structures of BiOX (X=F, Cl, Br, I) photocatalysts with and without semicore Bi 5d states", ***Journal of Computational Chemistry*** 0: 1-8, (2008).

[5] Mulliken,R.S., "Electronic population analysis on LCAO MO molecular wave functions-I***", J. Chem. Phys.*** 23: 1833, (1955).

[6] Segall, M.D., Pickard, C.J., Shah, R., and Payne, M.C., "Population analysis in plane wave electronic structure calculations", ***Mol. Phys***. 89: 571, (1996).

[7] Segall, M.D., Shah, R., Pickard, C.J., and Payne,M.C., " Population analysis of plane wave electronic structure calculations of bulk materials", ***Phys. Rev. B*** 54: 16317-16320, (1996).

[8] Kohn, W., and Sham, L.J., "Self-consistent equations including exchange and correlation effects", ***Phys. Rev***. 140: A1133-A1138, (1965).

[9] Ordejon, P., Artacho, E., and Soler, J. M., "Selfconsistent order-N density-functional calculations for very large systems", ***Phys. Rev. B*** (Rapid Common) 53: R 10441-R10444, (1996).

[10] Soler, J.M., Artaeho, E., Gole, J.D., Garsia, A., Ordejon, J. P., and Sanchez-portal, D., "The SIESTA method for ab initio order-N materials simulation", ***J. Phys: Condens Matter*** 14: 2745-2779, (2002).

[11] Ceperley, D.M., and Alder, M.J., "Ground state of the electron gas by a stochastic method", ***Phys. Rev. Lett***. 45: 566-569, (1980).

[12] Troullier, N. J., and Martins, L., "Efficient pseudopotentials for plane-wave calculations", ***Phys. Rev. B*** 43: 1993-2006, (1991).

[13] Sankey, O.F., and Niklewski, D.J., "Ab initio multicenter tight-binding model for molecular-dynamics simulations and other applications in covalent systems", ***Phys. Rev B*** 40: 3979-3995, (1989).

[14] Murnaghan, F.D., "The compressibility of media under extreme pressures", ***Proc. Nat. Acad. Sci.*** USA 30: 244-247, (1944).

[15] Li, L., Cao, R., Wang, Z., Li, J., and Qi, L., "Template synthesis of hierarchical Bi_2E_3 (E=S, Se, Te) core-shell microspheres and their electrochemical and photoresponsive properties", ***J. Phys. Chem. C*** 113: 18075-18081, (2009).

[16] Levine, Z.H., and Allan, D.C., "Linear optical response in silicon and germanium including self-energy effects", ***Phys. Rev. Lett.*** 63: 1719-1722, (1989).

[17] Philipp, H., and Ehrenreich, RH., "Optical properties of semiconductors", ***Phys. Rev***. 129: 1550-1560, (1963).

[18] Kovalev, O.V., Representations of the Crystallographic Space Groups. Irreducible Representations Induced Representations and Corepresentations, ***Amsterdam: Gordon and Breach*** (1965).

[19] Marton, L., "Experiments on low-energy electron scattering and energy losses", ***Rev. Mod. Phys.*** 28: 172-183, (1956).